Journal of Power and Energy Engineering, 2023, 11, 24-41
https://www.scirp.org/journal/jpee
ISSN Online: 2327-5901
ISSN Print: 2327-588X

# Corrosion-Based Integrity Analysis of Offshore Pipeline for Hydrocarbon Transportation

**David Emmanuel Udonsek[1], Daniel Tamonodukobipi[1], Victor Effiong Odokwo[2]**

[1]Department of Marine Engineering, Rivers State University, Port Harcourt, Nigeria
[2]Department of Marine Engineering, Akwa Ibom State University, Ikot Akpaden, Nigeria
Email: victorodokwo@aksu.edu.ng

**How to cite this paper:** Udonsek, D.E., Tamonodukobipi, D. and Odokwo, V.E. (2023) Corrosion-Based Integrity Analysis of Offshore Pipeline for Hydrocarbon Transportation. *Journal of Power and Energy Engineering*, **11**, 24-41.
https://doi.org/10.4236/jpee.2023.115002

**Received:** March 22, 2023
**Accepted:** May 28, 2023
**Published:** May 31, 2023



## Abstract

Conventional pipeline corrosion assessment methods result in failure pressure predictions that are conservative, especially for pipelines that are subjected to internal pressure and axial compressive stress. Alternatively, numerical methods may be used. However, they are computationally expensive. This paper proposes an analytical equation based on finite element analysis (FEA) for failure pressure prediction of a high toughness corroded pipeline with a single corrosion defect subjected to internal pressure and axial compressive stress. The equations were developed based on the weights and biases of an Artificial Neural Network (ANN) model trained with failure pressure from finite element analysis (FEA) of a high toughness pipeline for various defect depths, defect lengths, and axial compressive stresses. The proposed model was validated against actual burst test results for high toughness materials and was found to be capable of making accurate predictions with a coefficient of determination ($R^2$) of 0.99. An extensive parametric study using the proposed model was subsequently conducted to determine the effects of defect length, defect depth, and axial compressive stress on the failure pressure of a corroded pipe with a single defect. The application of ANN together with FEA has shown promising results in the development of an empirical solution for the failure pressure prediction of pipes with a single corrosion defect subjected to internal pressure and axial compressive stress.

## Keywords

Failure, Prediction, Marine Pipelines, Crude Oil, Subsea

## 1. Introduction

In the last three decades, an estimated 90,000 km of marine pipelines were installed for the transportation of hydrocarbons, with a yearly increment of about

5000 km [1]. A typical subsea pipeline system consists of submerged pipelines, flow lines, risers, jumpers, pipeline end termination (PLET), tie-in and spool connection parts, subsea Christmas trees/manifolds, flow control valves, umbilicals, pumps, etc. as shown in **Figure 1**. In subsea development, a multiphase composite of oil and gas is usually transported from the subsea well to a production platform without a separation process [2]. However, the integrity of these pipelines is often impaired by corrosion defects, dents, cracks, leaks, rupture, collapse and buckling [3] and this affects the integrity of pipelines.

Pipeline structural integrity is the ability of the pipeline to discharge its function effectively under prevailing service conditions over a specified duration without failure. Corrosion poses the most serious challenge to subsea pipeline operations. Despite seawater and process fluid containing carbon dioxide ($CO_2$) and hydrogen sulfide ($H_2S$), free water can cause severe corrosion problems in oil and gas pipelines [4]. Several previous studies have investigated corrosion-based integrity analysis of offshore pipelines, including studies by Li *et al.* [5], Tang *et al.* [6] and Wang *et al.* [7]. However, these studies have focused on specific aspects of corrosion-based integrity analysis, and there is a need for a comprehensive investigation into the effectiveness of these techniques in assessing the integrity of offshore pipelines.

This study looks into how well corrosion-based integrity analysis methods work for determining the integrity of offshore pipelines. With the help of several corrosion-based integrity analysis tools, the study will concentrate on pinpointing the major corrosion hotspots, estimating the remaining strength of the pipeline, and predicting its remaining useful life. To determine the damage accumulation, a time-dependent analysis of the structural properties and dynamic interaction with the external environment is imperative [8]. This work is aimed at analyzing corrosion-based integrity of offshore pipelines for crude oil conveyance in the oil-rich Niger Delta region of Nigeria and to add to the body of knowledge by revealing how well these methods work for determining the integrity of offshore pipelines.

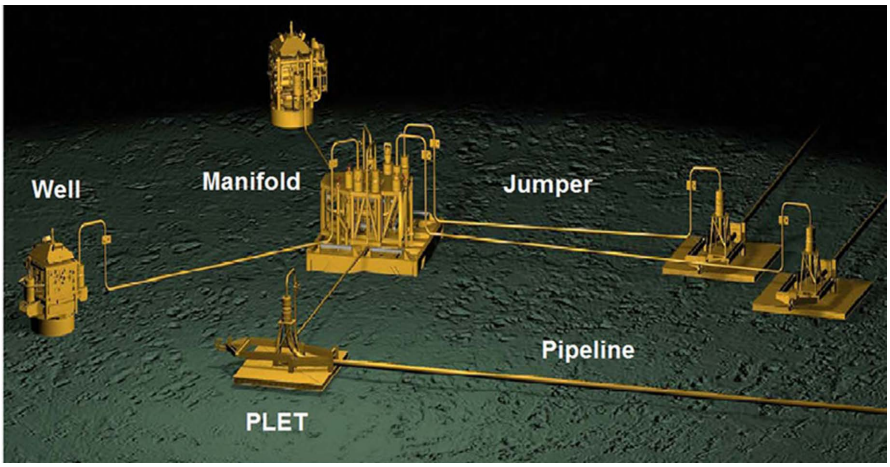


**Figure 1.** Schematic of a field development showing subsea pipeline.

## Mechanism of Corrosion

Steel materials corrode when exposed to a corrosive environment such as seawater or moist soil, in which the environment acts as the electrolyte. Corrosion occurs as an electrochemical reaction. When metal corrodes in seawater (an electrolyte), neutral metal atoms passes into solution by forming positively charged ions (oxidation: $\mathrm{M} \rightarrow \mathrm{M}^{n+}$) and producing excess electrons as given in $\mathrm{M} \rightarrow \mathrm{M}^{n+} + n\mathrm{e}^{-}$. Since the oxidation occurs at the anode, it is called Anodic reaction [9]. Anodic equations for some metals are represented below:

$$\left.\begin{array}{l} \mathrm{Cu} \rightarrow \mathrm{Cu}^{2+} + 2\mathrm{e}^{-} \\ \mathrm{Fe} \rightarrow \mathrm{Fe}^{2+} + 2\mathrm{e}^{-} \\ \mathrm{Zn} \rightarrow \mathrm{Zn}^{2+} + 2\mathrm{e}^{-} \\ \mathrm{Al} \rightarrow \mathrm{Al}^{3+} + 3\mathrm{e}^{-} \\ \mathrm{Cr} \rightarrow \mathrm{Cr}^{3+} + 3\mathrm{e}^{-} \\ \mathrm{Ni} \rightarrow \mathrm{Ni}^{3+} + 3\mathrm{e}^{-} \end{array}\right\} \quad (1)$$

The electrons lost from a metal are usually deposited on a non-metallic atom to form a negatively charged non-metallic ion. This reduction occurs at the cathode: hence it is called Cathodic reaction. The reduction reaction at the cathode can either be:

$$\mathrm{O}_2 + 2\mathrm{H}_2\mathrm{O} + 4\mathrm{e}^{-} \rightarrow 4\mathrm{OH}^{-} \quad (2)$$

Or reduction of hydrogen ions in acidic conditions

$$4\mathrm{H}^{+} + 4\mathrm{e}^{-} \rightarrow 2\mathrm{H}_2 \quad (3)$$

Or reduction of water at higher PH

$$4\mathrm{H}_2\mathrm{O} + 4\mathrm{e}^{-} \rightarrow 4\mathrm{OH}^{-} + 2\mathrm{H}_2 \quad (4)$$

In most cases, the corroded iron will be hydrated to form Hydrated ferric oxide (rust) as in Equation (5)

$$4\mathrm{Fe} + 3\mathrm{O}_2 + 2\mathrm{H}_2\mathrm{O} \rightarrow 2\mathrm{Fe}_2\mathrm{O}_3 \cdot 2\mathrm{H}_2\mathrm{O} \quad (5)$$

The common technique for minimizing marine corrosion is the application of coatings combined with cathodic protection (CP). The effective use of cathodic protection for carbon steel enables steel pipes, which has little natural corrosion resistance, to be used in corrosive environments such as seawater, acidic soils, and salt-laden concrete [10]. The choice and performance of an anode depend on its size and position in the galvanic series.

The anode utilization factor indicates the fraction of anode material that is assumed to provide cathodic protection current. Performance becomes unpredictable when the anode is consumed beyond a mass indicated by the utilization factor. The utilization factor of an anode is dependent on the detailed anode design, in particular the dimensions and location of anode cores. **Table 1** gives the anode utilization factor for different types of anodes [11].

Galvanic anodes for offshore application are generally based on either aluminium or zine. The generic type of anodes materials is basically chosen by the

project owner and specified in the conceptual design report. Aluminium-based anodes are preferred because of their electrochemical capacity. However, zinc based anodes have sometimes been taken to be more reliable for application in the marine sediments or internal compartments with high bacterial activity [12]. Since corrosion is the deterioration of a metal by electro-chemical reaction, a proper understanding of the electrochemical activity or Galvanic Series of metals as shown in Table 2 is imperative.

**Table 1.** Design utilization factors for different types of anodes [11].

| Anode Type | Anode Utilization Factor |
|---|---|
| Long l) slender stand-off | 0.90 |
| Long l) flush-mounted | 0.85 |
| Short 2) flush-mounted | 0.80 |
| Bracelet, half-shell type | 0.80 |
| Bracelet, segmented type | 0.75 |

**Table 2.** Galvanic series of metals.

| Electrode Reaction | Standard Potential, $\varphi^{\circ}$ in volts at 25˚C |
|---|---|
| $Au^{3+} + 3e^{-} = Au$ | 1.50 |
| $Pt^{2+} + 2e^{-} = Pt$ | ~1.2 |
| $Pd^{2+} + 2e^{-} = Pd$ | 0.987 |
| $Hg^{2+} + 2e^{-} = Hg$ | 0.854 |
| $Ag^{+} + e^{-} = Pt$ | 0.800 |
| $Cu^{+} + e^{-} = Cu$ | 0.521 |
| $Cu^{2+} + 2e^{-} = Cu$ | 0.342 |
| $2H^{+} + 2e^{-} = H_2$ | 0.000 |
| $Pb^{2+} + 2e^{-} = Pb$ | −0.126 |
| $Sn^{2+} + 2e^{-} = Sn$ | −0.136 |
| $Mo^{2+} + 2e^{-} = Mo$ | ~−0.2 |
| $Ni^{2+} + 2e^{-} = Ni$ | −0.250 |
| $Co^{2+} + 2e^{-} = Co$ | −0.277 |
| $Ti^{+} + e^{-} = Ti$ | −0.336 |
| $In^{3+} + 3e^{-} = In$ | −0.342 |
| $Cd^{2+} + 2e^{-} = Cd$ | −0.403 |
| $Fe^{2+} + 2e^{-} = Fe$ | −0.440 |
| $Ga^{3+} + 3e^{-} = Ga$ | −0.53 |
| $Cr^{3+} + 3e^{-} = Cr$ | −0.74 |
| $Zn^{2+} + 2e^{-} = Zn$ | −0.763 |

**Continued**

| | |
|---|---|
| $Cr^{2+} + 2e^- = Cr$ | −0.91 |
| $Nb^{3+} + 3e^- = Nb$ | ~−1.1 |
| $Mn^{2+} + 2e^- = Mn$ | −1.18 |
| $Zr^{4+} + 4e^- = Zr$ | −1.53 |
| $Ti^{2+} + 2e^- = Ti$ | −1.63 |
| $Al^{3+} + 3e^- = Al$ | −1.66 |
| $Hf^{4+} + 4e^- = Hf$ | −1.70 |
| $U^{3+} + 3e^- = U$ | −1.80 |
| $Be^{2+} + 2e^- = Be$ | −1.85 |
| $Mg^{2+} + 2e^- = Mg$ | −2.37 |
| $Na^{+} + e^- = Na$ | −2.71 |
| $Ca^{2+} + 2e^- = Ca$ | −2.87 |
| $K^{+} + e^- = K$ | −2.93 |
| $Li^{+} + e^- = Li$ | −3.05 |

## 2. Materials and Methods

### 2.1. Research Methods

The $CO_2$ induced corrosion of carbon-steel oil pipeline in the presence of liquid is affected by so many parameters. A slight change in one of these could significantly alter the corrosion rate. The following are the most common: Temperature, Partial pressure of $CO_2$, Fluid flow regime and velocity, PH value of transport liquid, Corrosion product concentration in solution ($FeCO_3$), Acetic acid concentration etc. Since corrosion-resistant alloys (e.g., 13% Cr steel and duplex stainless steel) are not economically viable for long-distance pipelines. It thus makes engineering sense that the desirable properties of other engineering material that can serve the same purpose be utilized [13], the material for the pipeline in consideration is carbon steel ASTM A36 grade with the following material properties with Subsea Transmission Pipeline characteristics shown below and in Table 3:

- Young Modulus, $E = 200$ GPa;
- Stress, $\sigma_y = 250$ MPa;
- Ultimate Tensile Stress, UTS = 400 - 550 MPa.

The corresponding temperature profile of the site considered is represented by Figure 2. Water depth of less than 500 m, located in the Niger Delta region of Nigeria is considered.

#### 2.1.1. Prediction of Corrosion Rate and Wear of Carbon Steel

Qin and Cui (2003) [14] corrosion model is used to demonstrate the corrosion rate and wear. This model and its variants are widely used to predict corrosion on general and specific cases. Equations (6) and (7) represent the corrosion

**Table 3.** Subsea transmission pipeline characteristics.

| Particulars | Parameters |
|---|---|
| Pipe size | 254 mm (10") |
| Pipe length | 3500 m (12 m is used for the analysis) |
| Nominal wall thickness | 18 mm |
| Internal diameter | 236 mm |
| Outer diameter | 272 mm |
| Pipe inlet pressure | 34.4 bar |
| Pipe inlet temperature | 89˚C - 95˚C |
| Operation time | 6 years |
| Pipe roughness | 0.04572 mm |
| Wall shear stress | 0.57 - 8.57 Pa |
| Standard used | BS31.3 |
| **Environment** | |
| Seawater temperature | 5˚C, 15˚C and 95˚C |
| Seawater average PH | 6.0 |
| Fluid type | Multiphase |
| Partial pressure of $CO_2$ | 5.92 - 7.28 bar |
| Gas velocity | 0.20 - 0.24 m/s |
| Liquid velocity | 0.44 - 2.13 m/s |

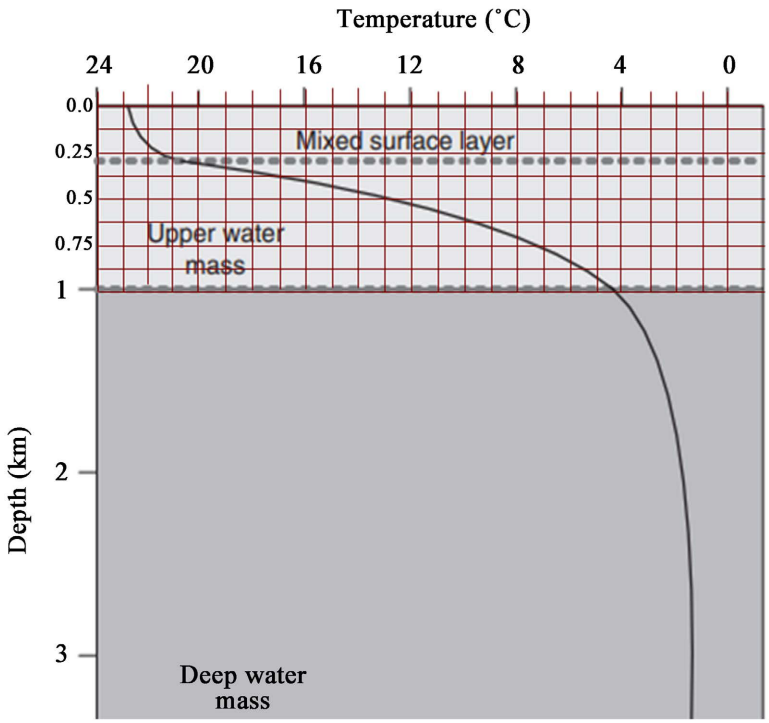


**Figure 2.** Hydrographic chart for depth against seawater temperature (Source: Uyeghe Stubb Offshore Pipeline Project, 1985).

models for corrosion rate and wear, respectively.

$$Cr(t) = d_{\infty}\frac{\beta}{\eta}\left(\frac{t-T_{St}}{\eta}\right)^{\beta-1}\cdot\exp\left\{-\left(\frac{t-T_{St}}{\eta}\right)^{\beta}\right\} \tag{6}$$

$$Cw(t) = d_{\infty}\left\{1-\exp\left[-\left(\frac{t-T_{St}}{\eta}\right)^{\beta}\right]\right\} \tag{7}$$

where: time is $0 \le t \le T_{St}$ and $T_{St} \le t \le T_L$.

$Cr(t)$ = corrosion rate at time "$t$", $Cw(t)$= corrosion wear at time "$t$", $d_{\infty}$ = Long term corrosion wastage of pipe thickness $d_{\infty} = d_{\max} + D_d$, $T_{St}$ = Instant at which corrosion is observed, $T_L$ = Life of the structure, $d_{\max}$ is the maximum wear in the distribution and $D_d$ is chosen as $\frac{d_{\max}}{100}$.

However, Equation (6) can be rewritten as:

$$-In\left(-In\left(1-\frac{d(t)}{d_{\infty}}\right)\right) = \beta In\eta - \beta In\left(t-T_{St}\right) \tag{8}$$

$$\text{If}\begin{cases} Y = -In\left(-In\left(1-\dfrac{d(t)}{d_{\infty}}\right)\right) \\ X = In\left(t-T_{St}\right) \\ A = \beta In\eta \\ B = -\beta \\ \eta = \exp\left(\dfrac{A}{\beta}\right) \end{cases}$$

Then, Equation (8) reduces to:

$$Y = A + BX \tag{9}$$

$\beta$, $\eta$, $d_{\infty}$ and $T_{St}$ are the four random parameters of the model corresponding to: $d_{\infty} = 1.8281$, $T_{St} = 1.40$, $\beta = 0.3915$ and $\eta = 1.5180$. Applying equation (9) using these values and by linear regression produces the line with: $A$= 0.1634 and $B$ = −0.3915.

Thus, the line is:

$$Y = 0.1634 - 0.3915X \tag{10}$$

From Equation (10), the random parameters for Equations (8) and (9) can be derived as:

$$\beta = -B = 0.3915 \text{ and } \eta = \exp\left(\frac{A}{\beta}\right) = \exp\left(\frac{0.1634}{0.3915}\right) = 1.5180$$

For this analysis, the effect of flow on sweet corrosion rate can be estimated using a resistance model as:

$$U_{cr}\frac{1}{\frac{1}{U_r}+\frac{1}{U_m}} \tag{11}$$

where: $U_{cr}$ represents the corrosion rate in mm/year, $U_r$ denotes the flow-independent reaction rate, $U_m$ represents the flow-dependent mass transfer rate.

For a multiphase turbulent flow in a pipeline, $U_m$ is dependent on the flow velocity and the liquid film thickness. It can be estimated as:

$$U_m = 2.45 \cdot \frac{U^{0.8}}{d^{0.2}} \cdot p_{CO_2} \tag{12}$$

where the partial pressure of $CO_2$ in bar, symbolised by $p_{CO_2}$ can be obtained using the relationship:

$$p_{CO_2} = \begin{cases} \dfrac{\text{mass flow of } CO_2 \text{ in the gas phase}(\text{kmole/h})}{\text{total mass flow in the gas phase}(\text{kmole/h})} \times P \\ \dfrac{\text{mole\% } CO_2(\text{g})}{100\%} \times P \end{cases} \tag{13}$$

### 2.1.2. Temperature and pH Dependencies of Corrosion Rate

The corrosion rate (CRt) in *mm/year* can be estimated more accurately by a set of temperature and pH dependent models which are expressed as follows:

For 20˚C ≤ $T$ ≤ 150˚C:

$$\text{CRt} = K_t \times f_{CO_2} \times f_{\text{pH}} \times \left(\frac{S}{19}\right)^{0.146+0.0324\log(f_{CO_2})} \tag{14}$$

For $T$ = 15˚C:

$$\text{CRt} = 0.36K_t \times f_{CO_2} \times f_{\text{pH}} \times \left(\frac{S}{19}\right)^{0.146+0.0324\log(f_{CO_2})} \tag{15}$$

For $T$ = 5˚C:

$$\text{CRt} = 0.36K_t \times f_{CO_2} \times f_{\text{pH}} \tag{16}$$

Temperature affects the kinetics of the corrosion process and surface temperature is a critical factor. When the surface temperature increases, the corrosion rate will rise sharply to the point at which evaporation of the electrolyte takes place. At this temperature, the corrosion rate will decrease quickly [15] [16]. The corrosion rate between temperatures can be obtained by linear interpolation. The corresponding corrosion constant $K_t$ and pH-function are given in **Table 4**. At high pressure, gases are not ideal, and their partial pressures can be corrected by a fugacity constant. The fugacity function of $CO_2$ pressure is expressed as:

$$f_{CO_2} = a \times p_{CO_2} \tag{17}$$

The fugacity coefficient is given as

$$a = \begin{cases} 10^{P\times(0.0031-1.4/T)} \rightarrow \text{for } P \le 250 \text{ bar} \\ 10^{250\times(0.0031-1.4/T)} \rightarrow \text{for } P \ge 250 \text{ bar} \end{cases} \tag{18}$$

Since water depths of less than 500 m and an average PH = 6.0 are considered, temperatures $T$ = 5˚C, $T$ = 15˚C and $T$ = 20˚C are implemented. The pH and fugacity functions corresponding to the chosen temperatures are calculated as:

**Table 4.** Corrosion constant for various temperatures.

| Temperature ˚C | $K_t$ |
|---|---|
| 5 | 0.42 |
| 15 | 1.59 |
| 20 | 4.762 |
| 40 | 8.927 |
| 60 | 10.695 |
| 80 | 9.949 |
| 90 | 6.250 |
| 120 | 7.770 |
| 150 | 5.203 |

For $T = 5^{\circ}\text{C}$: $f(\text{pH}=6) = 4.342 - (1.051\times 6) + (0.0708\times 6^2) = 0.5848$ and $K_t = 0.42$

$$f_{CO_2} = a \times p_{CO_2} = 2.983\times 10^{-10} \times 6.6 = 1.969\times 10^{-9}$$

where:

$$a = 10^{P\times(0.0031-1.4/T)} = 10^{34.4\times(0.0031-1.4/5)} = 2.983\times 10^{-10}$$

For $T = 15^{\circ}\text{C}$: $f(\text{pH}=6) = 4.986 - (1.191\times 6) + (0.0708\times 6^2) = 0.3888$ and $K_t = 1.59$

$$f_{CO_2} = a \times p_{CO_2} = 7.87\times 10^{-4} \times 6.6 = 5.194\times 10^{-3}$$

where:

$$a = 10^{P\times(0.0031-1.4/T)} = 10^{34.4\times(0.0031-1.4/15)} = 7.87\times 10^{-4}$$

For $T = 20^{\circ}\text{C}$: $f(\text{pH}=6) = 5.1885 - (1.2353\times 6) + (0.0708\times 6^2) = 0.3273$ and $K_t = 4.762$

$$f_{CO_2} = a \times p_{CO_2} = 4.996\times 10^{-3} \times 6.6 = 3.297\times 10^{-2}$$

where:

$$a = 10^{P\times(0.0031-1.4/T)} = 10^{34.4\times(0.0031-1.4/20)} = 4.996\times 10^{-3}$$

The fugacity coefficients are valid, since the operating pressure is 34.4 bar, that is $P \le 250$ bar.

### 2.1.3. The Remaining Strength Criteria of Corroded Pipeline

To determine the corroded pipe integrity, it is imperative for its remaining strength to be estimated. Some assessment parameters for corroded pipelines are: Allowable maximum length of defects, allowable maximum pressure for uncorroded pipelines and maximum safe pressure. Based on these, the predicted hoop stress level at failure of corroded pipe is approximated using Equation (19):

$$S_F = S_{\text{flow}}\left[\frac{1-A_R}{1-(A_R/M_F)}\right] \tag{19}$$

where: $S_{flow}$ is the flow stress of the material, $A_R$ is the area ratio and $A_R = A_{flaw}/A_0$, $A_{flaw}$ is the area of through thickness profile of flaw, $A_0$ is the area of uncorroded equivalence to flaw profile and $A_0 = L \times t$.

Similarly: $L$ is the maximum axial range of the defect, $T$ is the nominal wall thickness of the pipe, $D$ is the nominal diameter of the pipe and $M_F$ is the Folias factor, which is determined by:

$$M_F = \sqrt{1 + \frac{0.8 \times L^2}{D \times t}} \tag{20}$$

### 2.1.4. Allowable Maximum Length and Depth of Defect

The maximum allowable corroded length for a defect depth "$d$", nominal wall thickness "$t$", nominal diameter "$D$", and depth ratio ($d_R = d/t$) in the range of $0.1 < d_R < 0.8$, is estimated using Equation (21):

$$L_D = 1.12\sqrt{D \times t\left[\left(\frac{d_R}{1.1d_R - 0.15}\right)^2 - 1\right]} \tag{21}$$

By equating the maximum allowable operating pressure to the maximum allowable design pressure, the maximum allowable defect depth can be estimated as

$$\text{When } A \le 4 \quad d_{\max} = 1.5t\left[\frac{1-k}{1-k\sqrt{A^2+1}}\right] \tag{22}$$

$$\text{When } A > 4 \quad d_{\max} = t(1-k) \tag{23}$$

where: the pressure ratio, $k = \frac{p_{op.max}}{1.1p_{max}}$ and $A = 0.803\frac{L}{\sqrt{D \times t}}$.

However, when the safe maximum pressure is $P_{safe} < P_{max}$ and $A \le 4$, its value is given by Equation (24)

$$P_{safe} = 1.1P_{max}\left[\frac{3-2d_R}{3-2\frac{d_R}{\sqrt{A^2+1}}}\right] \tag{24}$$

Similarly, as $P_{safe} < P_{max}$ and $A > 4$, Equation (24) becomes

$$P_{safe} = 1.1P_{max}(1-d_R) \tag{25}$$

### 2.1.5. Effect of Corrosion on Structures

Integrity and strength capacity are the two critical design criteria considered for structural systems. Typically, structural capacity is a function of the cross-sectional dimensions of the structural member according to [17] as given in Equation (26).

$$R(t) = \sigma(A - p \cdot C(t)) \tag{26}$$

where: $C(t)$ is the corrosion loss as a function of time and $P$ is the perimeter of the area exposed to seawater. For plates in bending, with corrosion possible on each side of the plate, the bending resistance becomes

$$R(t) = K \cdot \sigma_b \left[ d(t) \right]^2 = K \cdot \sigma_b \left[ d_o - 2 \cdot C(t) \right]^2 \quad (27)$$

## 3. Results and Discussion

This section presents the analyzed results of corroded pipeline with corrosion defect subjected to pressure load and hydrostatic compressive stress. Data obtained from Turret Engineering Nig. Ltd are utilized to determine the parametric influence of varying defect depths, defect lengths, and hydrostatic compressive stresses as discussed in the following sections.

### 3.1. Loss of Pipeline Thickness with Time

Corrosion inhibitors may mitigate the rate of corrosion, but no subsea pipeline is 100% protected. The rate of corrosion may be high at the onset of corrosion when any protective layer is broken, as shown in Figure 3. The rate of depletion of the pipe thickness due to corrosion is continuous, except promptly mitigated. The analysis showed that the reduction in thickness during the first three years is 0.20 mm, while the last five years is 0.055 mm. indicating a gradual slowdown of the corrosion rate as the years of service increases which correlates with the prediction model produced by Qin and Cui [16].

### 3.2. Logarithmic Decay of Corrosion Rate with Time

The corrosion rate decreases logarithmically with time as indicated in Figure 4.

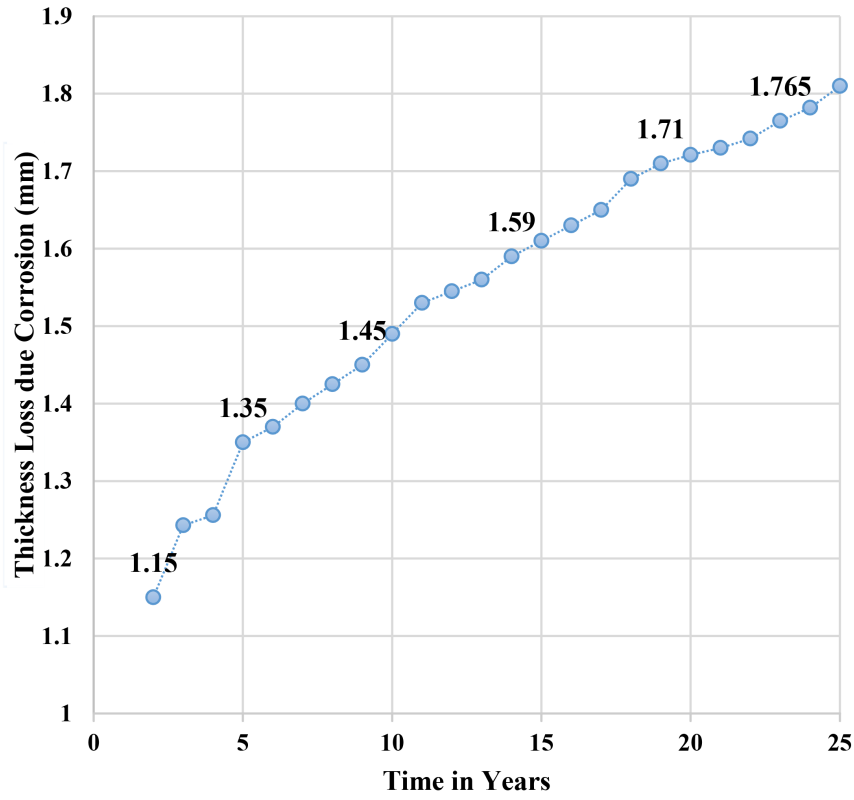


Figure 3. Loss of thickness due to corrosion on offshore pipeline.

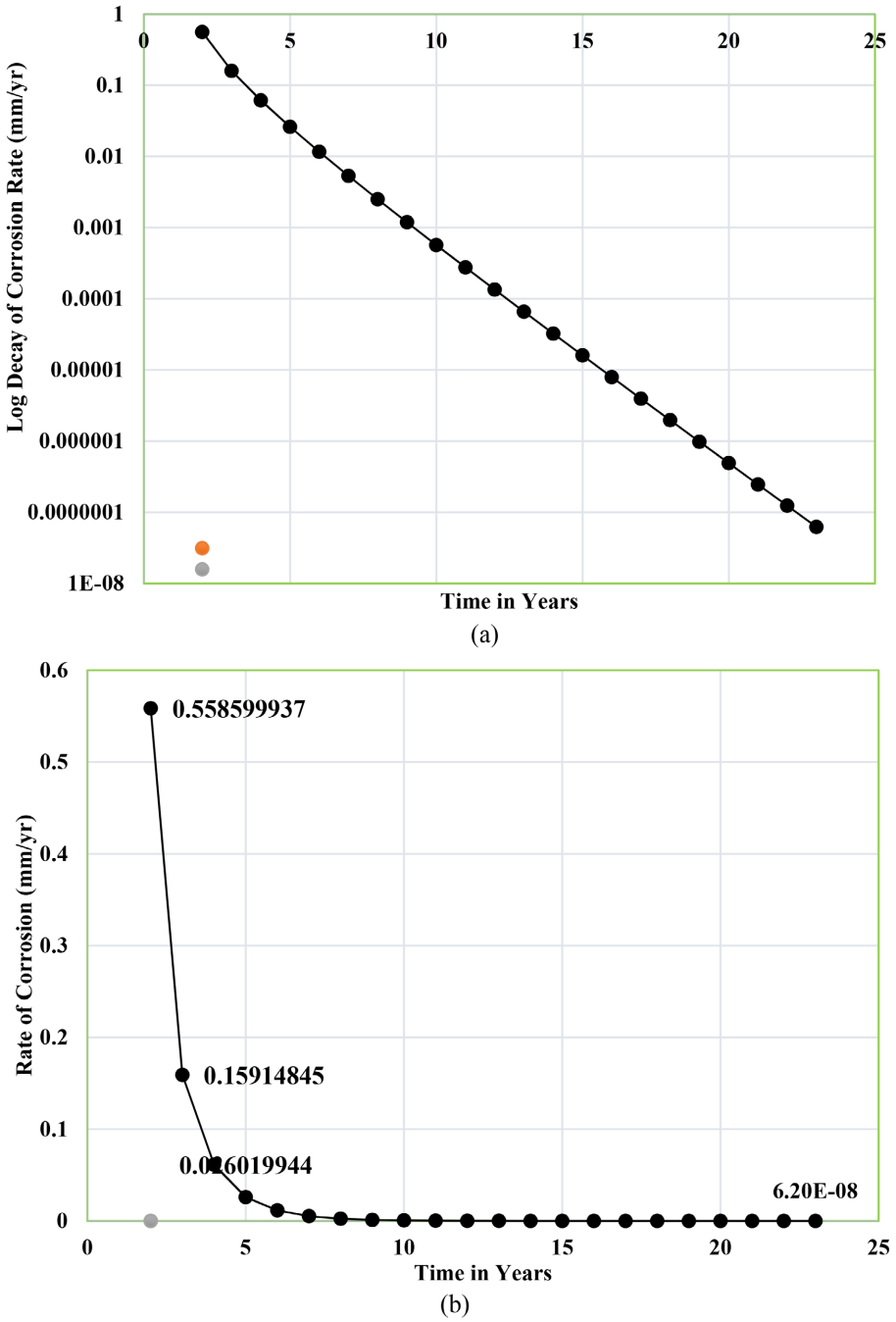


**Figure 4.** Corrosion rate decreases: (a) Logarithmically and (b) Asymptotically (Exponential Model).

This is true because the layers of corroded metal oxides tend to act as protective coating cover over the piping material. Their presence prevents the corrosive radicals from attacking the surface of the pipe below: thus, mitigating the rate of corrosion. Such reduction may not be obvious if surface erosion of metal oxide is prevalent. This agrees with the analysis given by Bia & Youde [2] based on time-dependent reliability analysis of corroded steel beam. This research's model gives a realistic standard prevents early failure pipe detection.

### 3.3. Asymptotic Decay of Corrosion Wear Rate with Time

Similar to corrosion rate, the corrosion wear rate decreases asymptotically along the x-axis as indicated in Figure 5. It shows that the wear rate is rapid at the beginning but grows lesser due to flow obstruction by scaly corroded materials and debris. The latter slow down the erosion effect, and hence the wear rate as the pipe ages in the water. The reliability and fitness for purpose of such pipeline are gradually eroded as a result of the combined effect of corrosion and wear. Compared to the model made available by David & Ramana [3], this model gives the closest output to corrosion wear and tear, therefore, can be used for wear and tear prediction for the aging corroded pipelines.

### 3.4. Corrosion Rate Dependence on Temperature

Figure 6 indicates that corrosion of subsea pipeline is sensitive to ambient water temperature. Until 15˚C, the corrosion rate curve is very gentle. Above that threshold temperature (15˚C), the corrosion curve is steeper. Considering the prediction model produced by Qin and Cui [16], this model provides an output that indicates the corrosion rate dependence on temperature and prevents early failure pipe detection. This implies that subsea pipeline in shallow water with higher ambient temperature would corrode faster than deep-water pipelines having lower ambient temperature.

### 3.5. Corrosion Defect Length Ratio and Depth Ratio

The effect of corrosion on subsea pipeline is continuous but differs in terms of its direction. Figure 7 presents corrosion defect length ratio and depth ratio. It is observed that the defect length ratio increases continuously with prolong service duration. Conversely, the defect depth ratio comes to a plateau after 20 years of

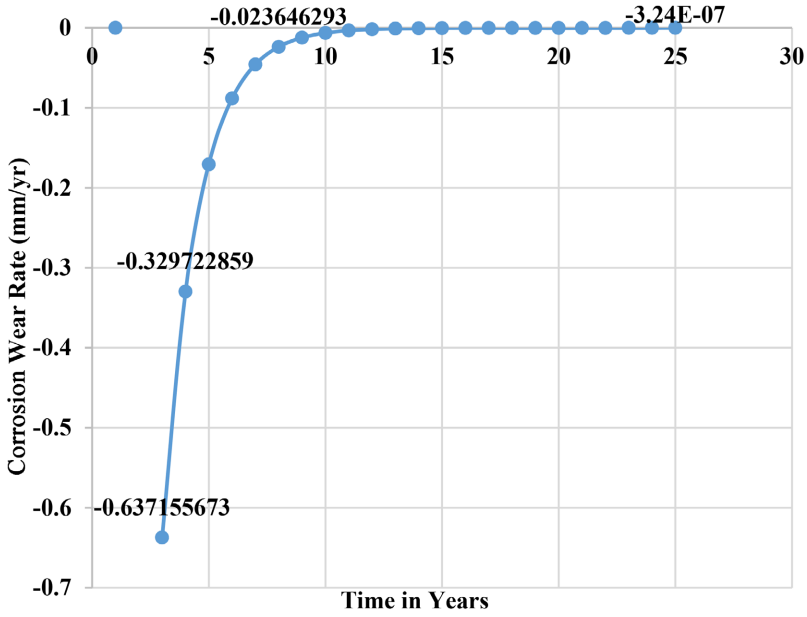


Figure 5. Corrosion wear rate decreases asymptotically with time.

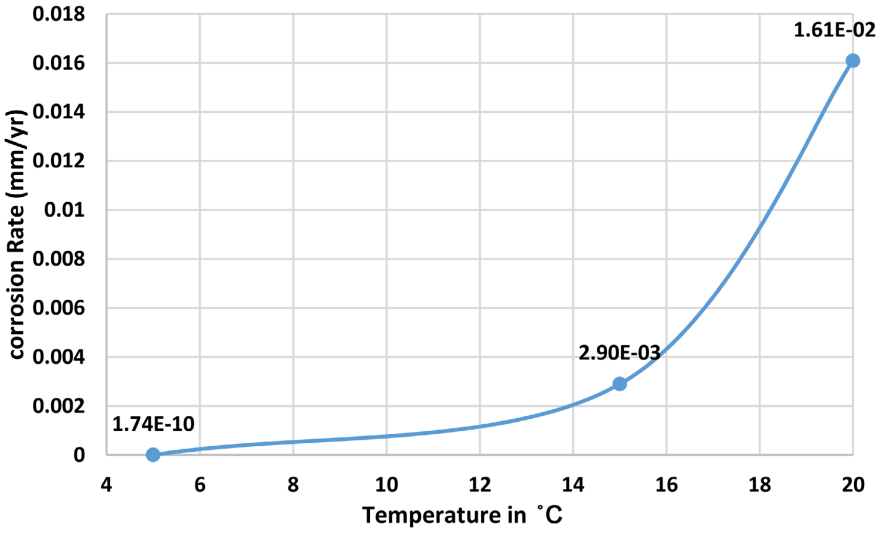


Figure 6. Sensitivity of corrosion rate to ambient seawater temperature.

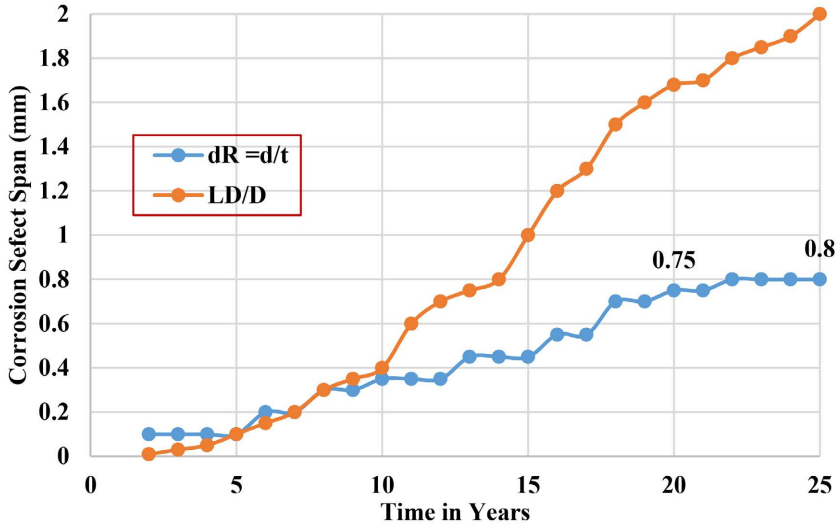


Figure 7. Variations of corrosion defect length ratio and depth ratio for service pipeline.

service. It implies that the radial growth of corrosion defect into the piping material stalls after several years. This can be elucidated by the formation of impervious corroded deposits on the surface of the pipeline, making it difficult for continuous incursion of corrosion. With this discrepancy, corrosion becomes more of surface effect than material penetrating defect. So, offshore structures can readily be maintained by cleaning off superficial corroded layers by sandblasting, wire-brushing, and thereafter coating with anti-rust paint.

### 3.6. Pipeline Failure Stress Ratio and Corrosion Length Ratio

Every engineering system has its design stress limit before failure. The ratio of the actual failure stress at any time in service to design failure stress is considered here as the failure stress ratio. This quantity is plotted alongside the corrosion length ratio against service period as shown in Figure 8. It is observed that

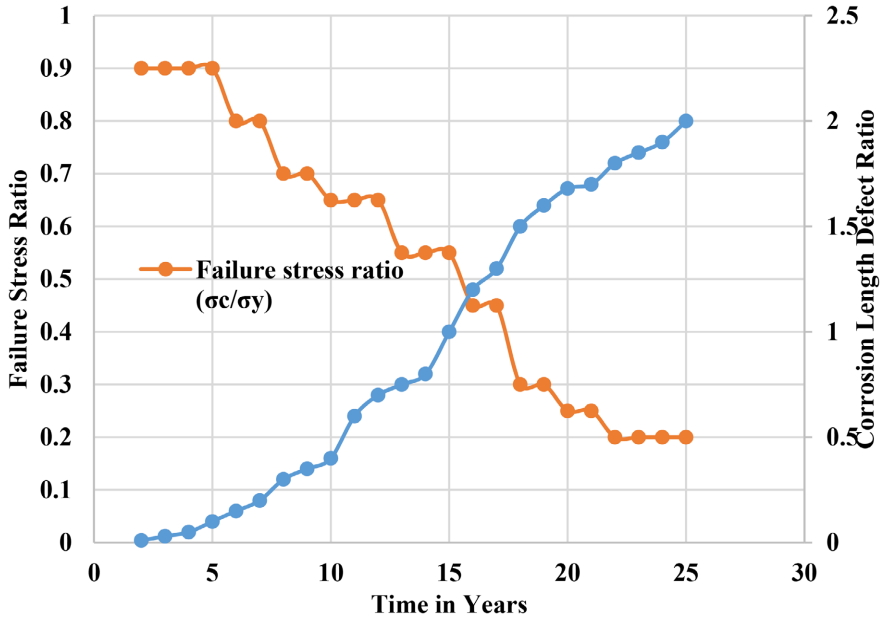


**Figure 8.** Relationship between failure stress ratio and corrosion defect length ratio of a subsea hydrocarbon pipeline under service loads.

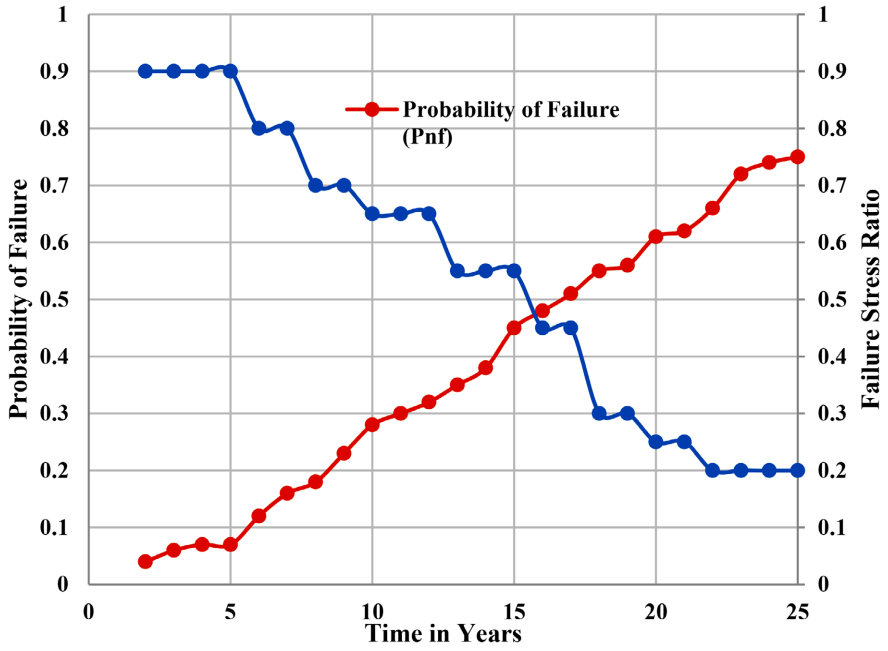


**Figure 9.** Relationship between probability of failure and failure stress ratio of a subsea hydrocarbon pipeline.

the failure stress ratio decreases from left to right as the corrosion defect length increases. Note that uninhibited corrosion of a subsea pipeline is prone to failure at stress level much below the design operating stress limit. For instance, in the analysis, from 2 to 5 years of operation, the pipeline coating is intact, and the failure stress ratio is 90% design stress limit. After 25 years, the failure stress ratio is 20% the design stress limit, if unmitigated. The pipeline could rupture un-

der loads well below the service load. To avoid such eventuality, subsea pipelines are adequately protected against corrosion.

### 3.7. Pipeline Failure Probability and Stress Ratio

In the current investigation, the integrity of a subsea pipeline is based on two indices, such as the failure stress ratio, and the probability of failure. The plots of these parameters are shown in **Figure 9**. The probability of failure increases with decrease in failure stress ratio. At failure ratio of 90%, the probability of failure is 4.0%. This means failure is unlikely as reliability and integrity are assured. However, after 17 years of operation, the failure stress ratio decreases to 45%, while the probability of failure becomes 51%. It implies greater tendency to fail and close monitoring is required. Eventually, after 25 years of operation, failure stress becomes 20%, while probability of failure is 75%. The pipeline at this stage is unreliable and dangerous for continuous usage. The investigation shows that the unprotected pipeline should not be used beyond 17 years, else failure due to rupture is imminent.

## 4. Conclusions

Subsea pipeline corrosion-induced failures have adversely affected pipeline integrity. The corrosion-based integrity analysis of offshore pipelines for hydrocarbon transportation is a crucial aspect of ensuring the safe and reliable operation of pipelines. Corrosion is a significant threat to offshore pipelines, and if left unchecked, it can result in catastrophic failures leading to environmental and economic damages.

The corrosion-based integrity analysis involves a systematic approach to identify, evaluate, and manage the risks associated with corrosion in offshore pipelines. This analysis includes the use of both canonical formulae and technical data from Uyeghe Stubb Offshore Pipeline Project. The author considers corrosion based on changing environmental factors, like temperature, pH, compositions of multiphase fluids, etc. under varying pressure loads and hydrostatic compressive stress. The results of the analysis provide critical information on the current condition of the pipeline; the rate of corrosion and the remaining life of the pipeline. This information helps operators to make informed decisions on maintenance and repair activities, ensuring the pipeline's continued safe operation. It offers crucial data that enables operators to choose wisely between maintenance and repair options and adhere to legal obligations. Therefore, to ensure the continuous safe operation of Uyeghe Stubb Offshore Pipeline, it is crucial to carry out regular corrosion-based integrity evaluations. The investigation shows that the pipeline should not be used beyond 17 years, when failure probability is 51%, else failure due to rupture is imminent. In conclusion, for durability and proper integrity management, subsea pipelines should be protected, monitored, and routinely maintained for abatement of corrosion and fit-for-purpose operation.

## Conflicts of Interest

The authors declare no conflicts of interest regarding the publication of this paper.

## References


[1] Garnelo, M. and Shanahan, M. (2019) Reconciling Deep Learning with Symbolic Artificial Intelligence: Representing Objects and Relations. *Current Opinion in Behavioral Sciences*, **29**, 17-23. https://doi.org/10.1016/j.cobeha.2018.12.010

[2] Bia, N., Shanhua, X. and Youde, W. (2019) Time-Dependent Reliability Analysis of Corroded Steel Beam. *KSCE Journal of Civil Engineering*, **24**, 255-265. https://doi.org/10.1007/s12205-020-1478-z

[3] David, V.S. and Ramana, M.P. (2010) A Theoretical Model for Metal Corrosion Degradation. *International Journal of Corrosion*, **2010**, Article ID: 279540. https://doi.org/10.1155/2010/279540

[4] Bhandari, J., Faisal, K., Rouzbeh, A., Vikram, G. and Roberto, O. (2015) Modelling of Pitting Corrosion in Marine and Offshore Steel Structures. *Journal of Loss Prevention in the Process Industries*, **37**, 39-62. https://doi.org/10.1016/j.jlp.2015.06.008

[5] Li, J., Yang, Y., Chen, G. and Qian, L. (2020) Corrosion Behavior and Integrity Analysis of Offshore Oil and Gas Pipeline in $CO_2$/$H_2S$ Environment. *Journal of Loss Prevention in the Process Industries*, **67**, Article 104191.

[6] Tang, X., Chen, X. and Gu, Q. (2018) A Comprehensive Integrity Assessment Method for Offshore Pipeline with Corrosion Defects. *Journal of Loss Prevention in the Process Industries*, **51**, 375-383.

[7] Wang, Y., Li, L. and Li, Y. (2019) Integrity Assessment of Corroded Offshore Pipeline Based on *In-Situ* and Laboratory Measurements. *Engineering Failure Analysis*, **106**, Article 104153. https://doi.org/10.1016/j.engfailanal.2019.104153

[8] Paik, J., Lee, M., Hawang, S. and Park, Y. (2003) A Time-Dependent Corrosion Wastage Model for the Structures of Single and Double Hull Tankers and FPSOs. *Marine Technology*, **40**, 201-217. https://doi.org/10.5957/mt1.2003.40.3.201

[9] Bai, Q. and Bai, Y. (2014) Force Model and Wave Fatigue. In: *Subsea Pipeline Design, Analysis, and Installation*, Gulf Professional Publishing, Houston, 365-384. https://doi.org/10.1016/B978-0-12-386888-6.00015-8

[10] Bai, Y. and Bai, Q. (2014) Corrosion and Corroded Pipelines. In: *Subsea Pipeline Integrity and Risk Management*, Gulf Professional Publishing, Houston, 3-25. https://doi.org/10.1016/B978-0-12-394432-0.00001-9

[11] DNV (1993) Cathodic Protection Design. Recommended Practice RP, DVN Corporate Headquarter, Oslo, Norway.

[12] DNV (2010) Cathodic Protection Design. Recommended Practice RP, DVN Corporate Headquarter, Oslo, Norway.

[13] Odokwo, V.E. and Ogbonnaya, E.A. (2019) Performance Optimization of Combined Gas and Steam Power Plant Using Artificial Neural Network. *Indian Journal of Engineering*, **16**, 35-45.

[14] Qin, S. and Cui, W. (2003) Effect of Corrosion Models on the Time Dependent Reliability of Steel Plated Element. *Marine Structures*, **16**, 15-34. https://doi.org/10.1016/S0951-8339(02)00028-X

[15] Pohlman, S.L. (1987) General Corrosion. In: Davis, J.R., Destefani, J.D., Frissell, H.J., Crankovic, G.M. and Jenkins, D.M., Eds., *Metals Handbook*, *Vol.* 13, *Corro-*

*sion*, 9th Edition, ASM International Handbook Committee.

[16] Guedes, C, Zayed, A. and Garbatov, Y. (2011) Effect of Environmental Factors on Steel Plate Corrosion under Marine Immersion Conditions. *Corrosion Engineering, Science and Technology*, **46**, 524-541. https://doi.org/10.1179/147842209X12559428167841

[17] Melchers R.E. (2005) The Effect of Corrosion on the Structural Reliability of Steel Offshore Structures. *Corrosion Science*, **47**, 2391-2410. https://doi.org/10.1016/j.corsci.2005.04.004